Manufacturing Letters 25 (2020) 64–69

Contents lists available at ScienceDirect

Manufacturing Letters

journal homepage: www.elsevier.com/locate/mfglet

Letters

Effect of weld power and interfacial temperature on mechanical strength and microstructure of carbon steel 4130 fabricated by ultrasonic additive manufacturing

Tianyang Han [a,1], Chih-Hsiang Kuo [b,1], Niyanth Sridharan [c], Leon M. Headings [a], Sudarsanam S. Babu [b,d], Marcelo J. Dapino [a,*]

[a] Center for Ultrasonic Additive Manufacturing, Department of Mechanical and Aerospace Engineering, The Ohio State University, Columbus, OH 43210, USA
[b] Department of Mechanical, Aerospace, and Biomedical Engineering, University of Tennessee, Knoxville, TN 37996, USA
[c] Oak Ridge National Laboratory, Oak Ridge, TN 37830, USA
[d] Energy and Transportation Science Division, Oak Ridge National Laboratory, Oak Ridge, TN 37831, USA

ARTICLE INFO

Article history:
Received 29 December 2019
Received in revised form 10 June 2020
Accepted 13 July 2020
Available online 30 July 2020

Keywords:
Ultrasonic additive manufacturing
Cobalt-chromium coated sonotrode
4130 carbon steel
Shear strength
Fractography

ABSTRACT

Ultrasonic additive manufacturing (UAM) is a solid-state 3D printing technology. Steels can be welded with UAM at reduced ultrasonic power, achieving half the shear strength of bulk material. A higher weld power is demonstrated by using a cobalt-based sonotrode coating, achieving shear strengths comparable to bulk 4130 material. In-situ temperature measurements and fracture surface analyses indicate that higher power input promotes metallurgical bonding through softening and increased plastic deformation. Carbides and ferrite are found at 1 μm scale at key weld interfaces; no martensite is found due to an increase in critical transformation temperatures associated with high heating rates.

1. Introduction

Ultrasonic additive manufacturing (UAM) is a solid-state additive manufacturing process that produces near net shape parts from metal foil feedstock [1]. Certain UAM systems integrate ultrasonic metal welding and computer numerical control (CNC) machining capabilities, which enable them to create parts with arbitrary internal features and unique geometries. During welding, shear strains produced by the ultrasonic (20 kHz) transverse vibration, combined with a force normal to the metal foil feedstock, create localized plastic deformation and form metallurgical bonds at the interface. Even though UAM welding of relatively soft alloys such as Al 6061 [2–4] and Cu 1100 [5] has been extensively investigated, UAM welding of high strength steels presents challenges [6–8]. Fabrication of UAM steel builds requires increased process temperature or increased ultrasonic weld power, where increased process temperature reduces the yield strength of the material and increased weld power induces intensified high strain rate deformation [9]. However, currently both the power and temperature inputs are restricted by practical limits. When ultrasonic power input is increased, the top of the steel foil tends to weld to the sonotrode due to galling, a form of adhesive wear. To avoid this phenomenon, the power input must be restricted, which limits the resulting strength of UAM 4130 steel builds. Even though a recent study has shown that increasing baseplate temperature improves UAM steel weld quality, commercial UAM systems are typically limited to baseplate temperatures under 204 °C (400 °F) [6]. A baseplate temperature of 204 °C is not sufficient to achieve a weld with shear strength comparable to that of bulk steel. Therefore, post heat treatment methods such as hot isostatic pressing (HIP) have been investigated to improve weld strength [8]. Considering the extra cost and time associated with HIP, methods to avoid HIP and achieve UAM welds with sufficient strength are desired.

The premise of this study is that increasing weld power improves the shear strength of as-welded UAM 4130 steel. A cobalt-based hard-facing alloy coated sonotrode is used to increase the galling threshold and allow a higher power input. Exact details on the composition and development of the coating are provided in two recent studies [10,11]. Previous research has shown that cobalt-based alloys can effectively suppress galling by preventing strain

* Corresponding author.
E-mail address: dapino.1@osu.edu (M.J. Dapino).
[1] Both authors contributed equally to this manuscript.

https://doi.org/10.1016/j.mfglet.2020.07.006
2213-8463/

localization at the contact surface [12]. The high galling resistance of cobalt is attributed to its high strain hardening ability, which allows significant plastic deformation to be imposed on the steel foils.

Since the mechanical power during plastic deformation can be divided into stored strain energy that is spent on actual deformation and heat that is dissipated to the surroundings by a constant fraction for a certain metal, both the strain energy and heat increase as the power input increases [13,14]. Because the thermal conductivity of the coated sonotrode is only half that of the uncoated sonotrode, the heat loss through the sonotrode during welding should be lower. With higher heat inputs and lower heat losses, a higher interfacial temperature is anticipated. As the interfacial temperature increases, the yield strength of 4130 steel will decrease [15]. It becomes easier to plastically deform asperities and form metallurgical bonding at the welding interface. Therefore, with increased plastic work and decreased yield strength at the welding interface during welding, the resulting weld strength of UAM 4130 is expected to increase.

2. Experimental methods

In this study, all UAM samples were manufactured using a 9 kW Fabrisonic SonicLayer 4000 UAM system. Two control builds were fabricated using an uncoated tool steel (18Ni grade 350) sonotrode (UCS), while another build was made using a cobalt-chromium coated tool steel (18Ni grade 350) sonotrode (CS). The CS and UCS have the same geometry and resonate at the same nominal frequency (20 kHz). Each sample was made from nine layers of 0.127 mm (0.005 in) thick, 25.4 mm (1 in) wide annealed 4130 steel foils and 6.35 mm (0.25 in) thick low carbon steel baseplates (ASTM A36 or AISI 4130). The welding parameters are summarized in Table 1. Note that the high welding parameters that work with the CS cannot be used with the UCS without damaging both the sonotrode and the build. Each control build is referred to as "UCS" whereas builds made using the coated sonotrode are denoted "CS". The HIP process was conducted on one of the UCS builds ("UCS-HIP"). The HIP treatment was carried out with a temperature of 1000 °C, an argon pressure of 200 MPa, and a duration of 4 h.

An OMEGA Type K AWG40 thermocouple (0.080 mm tip diameter) was used to measure the temperature at the interface of the baseplate and the first foil. The time constant of the thermocouple is 0.1 s. A thermocouple amplifier SEN30101 produced by Playing With Fusion, Inc was used to amplify the voltage signal generated by the thermocouple. The tolerance of this temperature measurement system including the thermocouple and data acquisition system is ±3 °C. Temperature data was collected at 5 kHz. The experimental setup is shown in Fig. 1(a). A thermocouple was placed through a 1.5 mm hole in the baseplate and the tip was bent onto the top surface. Temperature was measured while the first layer of foil was welded onto the baseplate using the coated sonotrode. To help understand the effect of temperature on microstructural changes, the continuous cooling transformation (CCT) diagram, equilibrium lower critical temperature (Ac1), and upper critical temperature (Ac3) were calculated using JMatPro.

A customized shear test method was used to characterize the mechanical strength of the baseplate and first foil interface of UAM builds. Five shear test samples for UCS and UCS-HIP and three shear test samples for CS treatment conditions were cut out from UAM builds, prepared following the procedure described in a previous study [6], and then tested on an MTS C43.504 50 kN load frame. In addition to mechanical testing, microstructural analyses were performed with scanning electron microscopy (SEM). The UAM sample that was made with the coated sonotrode was prepared according to standard metallographic procedures and then etched with 2% Nital. A micrograph of the weld interface was taken on a JEOL 6500 FEG SEM with an accelerating voltage of 10 keV and a working distance of 8 mm. Post-shear micrographs of the fracture surface were taken on a Zeiss EVO MA15 SEM with an accelerating voltage of 20 keV and a working distance of 8 mm.

Table 1
Process parameters used to weld UAM 4130.

Parameters	UCS/UCS-HIP	CS
Normal force (N)	6500	6500
Vibration amplitude (μm)	32.4	38.8
Weld speed (mm/s)	17	21
Baseplate temperature (°C)	204	204
Sonotrode	uncoated	coated

3. Results and discussion

The interfacial temperature profile was measured during welding of the first foil layer onto the baseplate. The total weld length is 76.2 mm and the thermocouple was placed 12.9 mm away from the starting point, along the centerline of the weld interface. Previous research, including experimental measurements and simulations, have shown that the temperature profile of the UAM process is not sensitive to the location of the thermocouple along the weld [16,17]. The contact area width of the sonotrode pressing on the foil is estimated to be about 2.54 mm based on empirical evidence [18]. During time period *a* (0 s to 0.44 s), as shown in Fig. 1(b), the coated sonotrode pressed the foil against the baseplate, started to weld, and approached the thermocouple location. A slight drop of the temperature from the preset point of about 200 °C was recorded as the cooler foil (at room temperature) absorbed heat from the baseplate. Then, when the sonotrode reached a location that is about 3.6 mm before the thermocouple and formed a weld, temperature started to rise. The peak temperature was reached at the end of period *b* (0.44 s to 0.67 s), when the sonotrode had moved across the thermocouple and the trailing edge of the sonotrode-foil contact patch reached the thermocouple. The sharp increase in temperature is believed to be caused by the frictional heat and plastic deformation during welding [19]. During time period *c* (0.67 s to 3.6 s), when the sonotrode moved further away from the thermocouple location after the weld, the weld area cooled down through conductive and convective heat loss. According to the measurement, the peak interfacial temperature is 855 °C [2] for this CS sample, while the typical peak temperature range for welding different UCS samples is from 522 °C to 563 °C. [3] Since the peak interfacial temperature for the CS sample is above the 4130 steel equilibrium Ac3 of 801 °C, a body centered cubic (BCC) ferrite to face centered cubic (FCC) austenite phase transformation is expected. As shown in the CCT diagram in Fig. 1(c), if the cooling rate is higher than 100 °C/s, as is the case during the UAM process (about 900 °C/s for the first 0.5 s), an austenite to martensite phase transformation is expected to occur. We thus search for evidence of BCC martensite in the UAM 4130 that is made using the coated sonotrode.

However, as shown in Fig. 2(a), an SEM image of the interface between the baseplate and first foil, where the temperature is measured, shows only carbides and ferrite at 1 μm scale. The fact that the microstructure of the interface is not fully martensitic could be explained by the increase of Ac1 and Ac3 due to the high heating rate. As reported in a study by Lolla et al. [20], the rapid heating rate (>400 °C/s) during flash processing of AISI 8620 steel increases Ac1 from 702 °C to 930 °C and Ac3 from 806 °C to 1050 °C. Since the UAM process has a similar heating rate, ferrite

[2] With nonlinearity correction applied per the thermocouple amplifier's manufacturer specification.

[3] The temperature measurements are shown in the supplementary document.

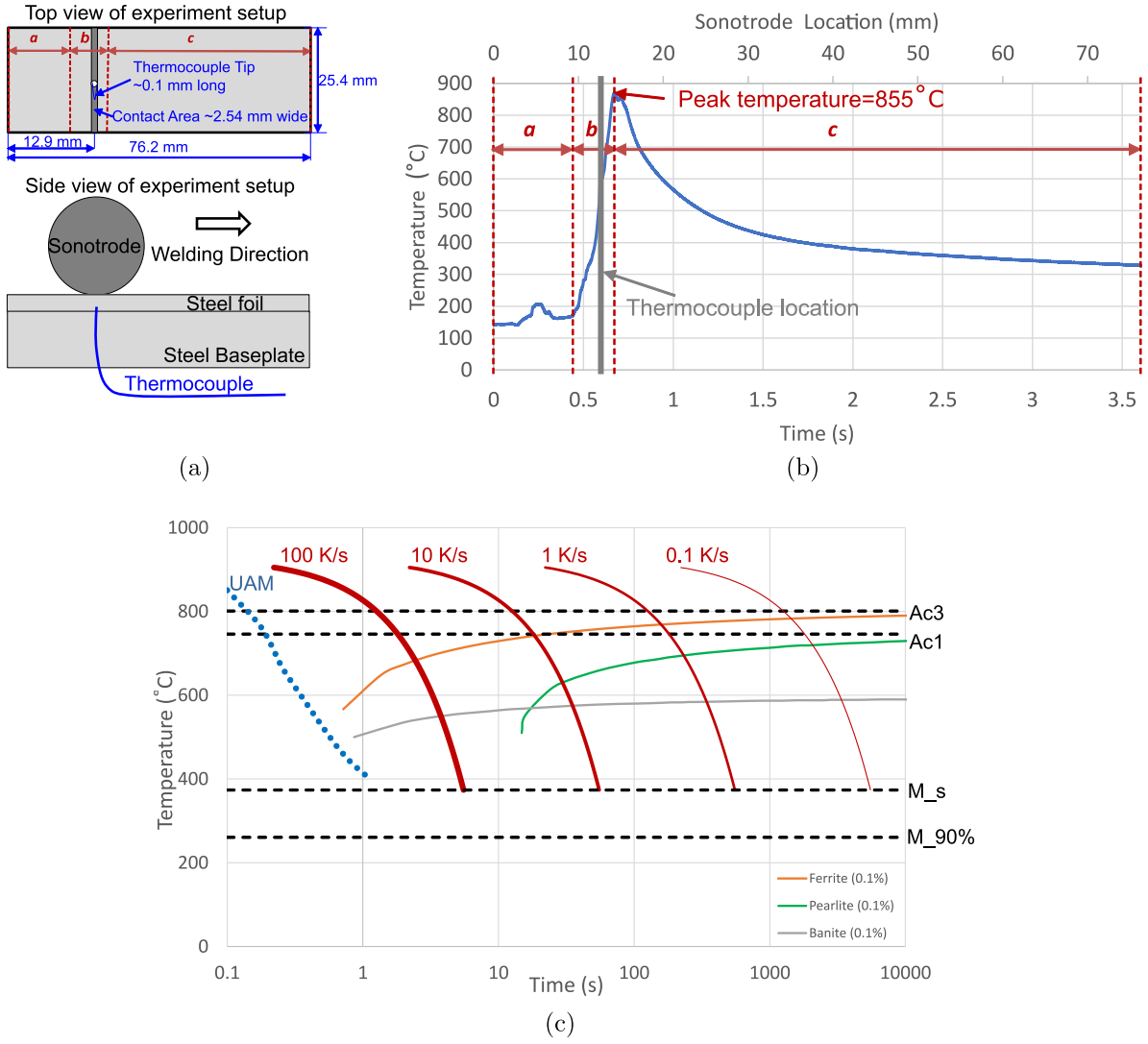

Fig. 1. (a) Temperature measurement setup showing the embedded thermocouple, (b) interfacial temperature measurement profile while the first layer of steel foil was welded onto the baseplate using the coated sonotrode, and (c) continuous cooling transformation (CCT) diagram of 4130 steel including the UAM cooling rate for comparison.

and carbides are expected at the interface. Due to the limited spatial resolution of SEM, a submicron size martensitic structure could not be observed. It is noted that martensite is found at the interface between the eighth and ninth layers of foil as shown in Fig. 2(b). This phenomenon may be caused by the high temperature that the sonotrode reaches after continuous welding and heating. Microstructural defects, including cracks and voids at weld interfaces in UCS builds, were identified and investigated in two previous studies [6,8] (see Fig. 3).

As summarized in Table 2, the average power input per unit area is 2695 W/m^2 for CS samples compared with 2066 W/m^2 for UCS samples. The average shear strength of CS samples is 549 MPa, while the shear strength is 186 MPa for UCS samples and 456 MPa for UCS-HIP samples. Both CS and UCS-HIP samples give an average shear strength comparable to that of bulk 4130 steel. The average shear strength of CS samples is 195% greater than that of UCS samples and 20% greater than that of UCS-HIP samples. The standard deviation of the CS builds is between that of UCS and UCS-HIP builds. Compared to HIP, fabrication using the coated sonotrode offers the advantage of avoiding an extra post-processing step. The variations in CS shear samples cut from the same CS builds may be caused by non-uniform heat input. Improvement of local welding variation may be achieved by optimizing the heating and cooling rate during the welding process. It is proposed that the higher strength of CS samples fabricated with a higher average power input is attributed to increased plastic deformation, which is caused by the reduction of the yield strength of 4130 at elevated process temperatures (still below melting temperature) and the increase of shear strain at the interface. [4]

To characterize the fracture surface failure types, a point count method [6] was used. Ten randomly located SEM images were taken for each condition and each SEM image was then evenly divided into a grid with 117 cells. Each cell was attributed one of four failure features based on surface morphology including brittle failure, machined surface, flow, and ductile failure. The area fraction of each failure feature for different treatment conditions is presented in Table 3. The definition for each failure feature is defined in a previous study [6]. Generally, a larger ductile area fraction indicates a better weld. As expected, compared with UCS samples, CS 4130 samples have much larger ductile areas and smaller brittle, flow, and machined areas, which indicates that stronger metallurgical bonding is achieved. Compared with UCS-HIP samples, CS 4130

[4] The average power per unit area is calculated by dividing the total energy input by the product of the welding time and the welding area. The total energy is calculated by integrating measured power over time.

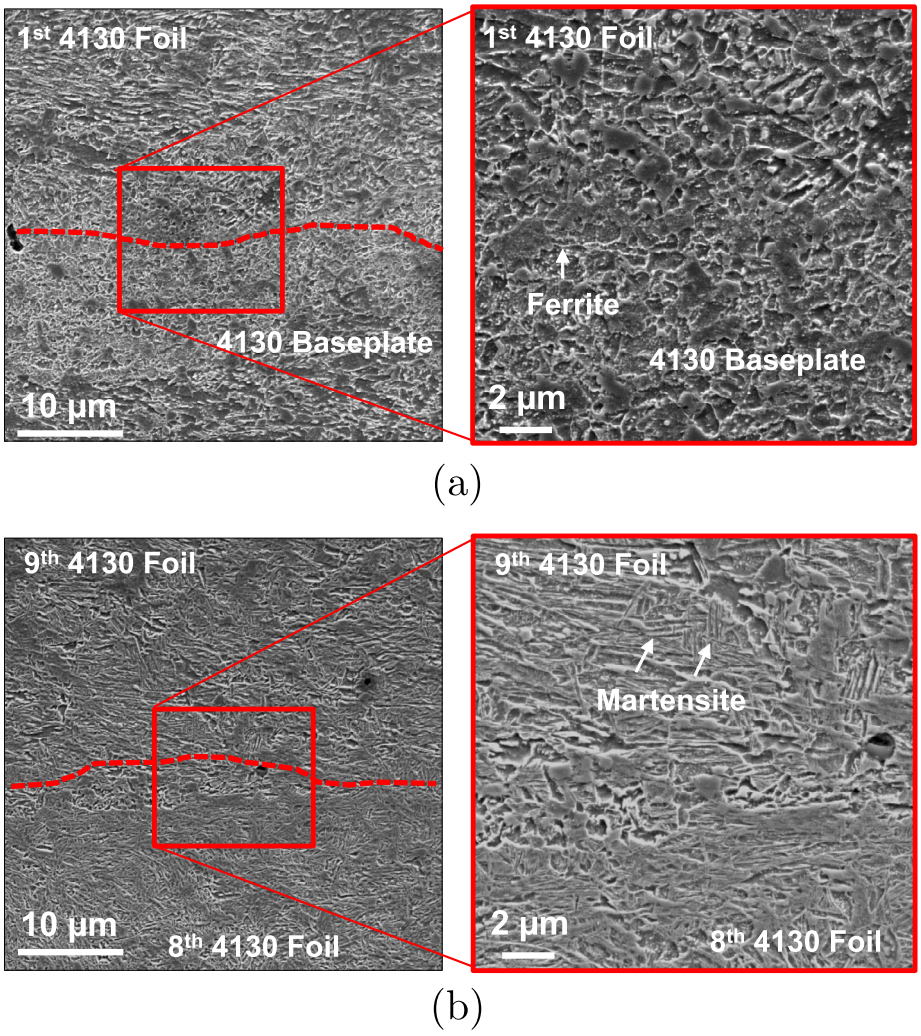

Fig. 2. Representative SEM images of (a) UAM interface region between the baseplate and first layer of foil and (b) UAM interface region between the eighth and ninth layers of foil. As shown in the insets on the right, only carbides and ferrite are found for the interface region in (a) and martensite is found for the interface region in (b). The interface location is determined from the contrast of surrounding area at lower magnification (not shown). The approximate interface locations are marked with red dotted lines in the images.

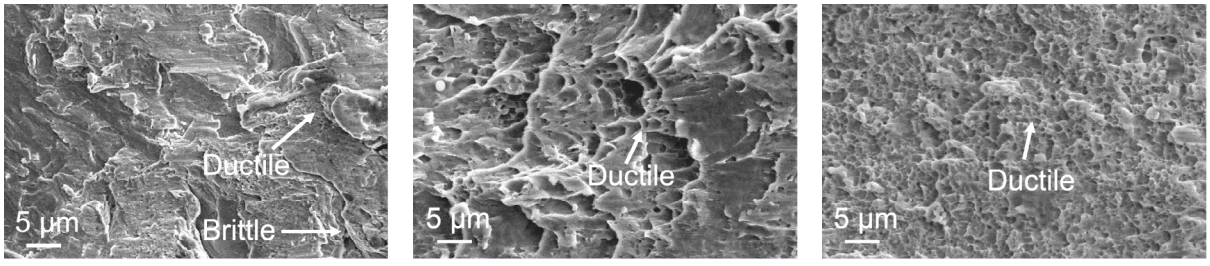

Fig. 3. SEM images of the post-shear fractured surface of samples (a) UCS 4130, (b) UCS-HIP 4130, and (c) CS 4130.

Table 2
Average ultimate shear strength of UAM 4130 steel.

Condition	UCS 4130	UCS-HIP 4130	CS 4130	Bulk 4130 [21]
Shear strength (MPa)	186	456	549	340∼640
Standard dev. (MPa)	61	10	26	N/A
Sonotrode	uncoated	uncoated	coated	N/A
Average power per unit area (W/m^2)	2066	2066	2695	N/A

Table 3
Area fraction of the failure features presented on the fracture surface.

Failure feature	UCS 4130	UCS-HIP 4130	CS 4130
Brittle failure	36.7%	1.5%	17.8%
Machined surface	28.3%	7.6%	16.3%
Flow	31.2%	26.4%	7.2%
Ductile failure	3.8%	64.5%	58.7%

samples have slightly smaller ductile areas and larger brittle and machined areas, which explains the variation between the shear samples. The results are consistent with the shear test results.

Overall, these results demonstrate that increasing weld power improves the shear strength of as-welded UAM 4130. However, similar to ultrasonic metal welding [22,23], an upper weld power threshold is expected for UAM, beyond which the weld strength decreases as the weld power increases. Several factors may contribute to this weld strength decrease. First, excessive plastic deformation at the weld interface may lead to increased void density and decreased strength [22]. Second, interfacial temperature increases as weld power increases. Beyond a certain weld power, residual stress formed due to thermal expansion and contraction of material during welding may exceed the yield strength of the material and cause localized delamination. Third, fatigue due to cyclic shear force at the weld interface, which is produced by the ultrasonic vibrations, is expected to become significant at high weld power and may cause cracking or delamination. Investigating these factors in detail and identifying upper power thresholds for each will be the focus of future work.

4. Conclusions

In this study, the effect of increased weld power on the mechanical strength of as-welded UAM steel has been investigated. Applying 2695 W/m^2 with a cobalt-chromium coated sonotrode achieves an average shear strength of 549 MPa, which is comparable to that of bulk 4130 material. This represents a 195% improvement over the shear strength of 186 MPa for samples fabricated with 2066 (W/m^2) using an uncoated steel sonotrode without post-processing and a 20% improvement over the shear strength of 456 MPa for HIP-treated samples. A point count analysis method with SEM was used to quantify post shear fracture surface features and the measurements are consistent with the shear test results. An in situ thermocouple temperature measurement method was used to monitor the interfacial temperature changes and a peak temperature of 855 °C was recorded with the coated sonotrode, which indicates significant softening of the 4130 steel. This softening and increased plastic deformation caused by higher power input lead to the weld quality improvement of UAM 4130. Even though the peak interfacial temperature is beyond the upper critical temperature (Ac3) of 801 °C for 4130 steel, a fully martensitic structure is not observed at the interface between the baseplate and the first layer of foil. This is attributed to an increase in lower critical temperature (Ac1) and upper critical temperature (Ac3) due to the high heating rate (>400 °C/s) during UAM welding of steels.

Declaration of Competing Interest

The authors declare that they have no known competing financial interests or personal relationships that could have influenced the work reported in this paper.

Acknowledgements

Financial support for this project is provided by the Government of Israel, Ministry of Defense PO No. 444080151. The authors want to thank Fabrisonic LLC. for providing the cobalt-chromium sonotrode and American Isostatic Presses, Inc. for performing the HIP treatments used in this study. One of the authors (Niyanth Sridharan) wishes to acknowledge the U.S. Department of Energy, Office of Energy Efficiency and Renewable Energy, Advanced Manufacturing Office, Technical Collaborations Program. This manuscript has been authored by UT-Battelle, LLC under Contract No. DE-AC05-00OR22725 with the U.S. Department of Energy. The United States Government retains and the publisher, by accepting the article for publication, acknowledges that the United States Government retains a nonexclusive, paid-up, irrevocable, worldwide license to publish or reproduce the published form of this manuscript, or allow others to do so, for the United States Government purposes. The Department of Energy will provide public access to these results of federally sponsored research in accordance with the DOE Public Access Plan (http://energy.gov/downloads/doe-public-access-plan).

Appendix A. Supplementary data

Supplementary data associated with this article can be found in the online version at https://doi.org/10.1016/j.mfglet.2020.07.006.

References

[1] Graff K, Short M, Norfolk M. Very high power ultrasonic additive manufacturing (VHP UAM) for advanced materials. In: Solid freeform fabrication symposium, Austin, TX.
[2] Gussev MN, Sridharan N, Thompson Z, Terrani KA, Babu SS. Influence of hot isostatic pressing on the performance of aluminum alloy fabricated by ultrasonic additive manufacturing. Scr Mater 2018;145:33–6.
[3] Wolcott PJ, Hehr A, Dapino MJ. Optimized welding parameters for Al 6061 ultrasonic additive manufactured structures. J Mater Res 2014;29:2055–65.
[4] Guo H, Gingerich MB, Headings LM, Hahnlen R, Dapino MJ. Joining of carbon fiber and aluminum using ultrasonic additive manufacturing (UAM). Compos Struct 2019;208:180–8.
[5] Sriraman M, Babu SS, Short M. Bonding characteristics during very high power ultrasonic additive manufacturing of copper. Scr Mater 2010;62:560–3.
[6] Han T, Kuo CH, Sridharan N, Headings LM, Babu SS, Dapino MJ. Effect of preheat temperature and post-process treatment on the microstructure and mechanical properties of stainless steel 410 made via ultrasonic additive manufacturing. Mater Sci Eng: A 2020;769:138457.
[7] Kuo CH, Sridharan N, Han T, Dapino MJ, Babu SS. Ultrasonic additive manufacturing of 4130 steel using Ni interlayers. Sci Technol Weld Joining 2019;24:382–90.
[8] Levy A, Miriyev A, Sridharan N, Han T, Tuval E, Babu SS, Dapino MJ, Frage N. Ultrasonic additive manufacturing of steel: method, post-processing treatments and properties. J Mater Process Technol 2018;256:183–9.
[9] Wolcott PJ, Dapino MJ. Ultrasonic additive manufacturing. In: Additive Manufacturing Handbook: Product Development for the Defense Industry. Florida: CRC Press/Taylor and Francis Boca Raton; 2017.
[10] Sridharan N, Dehoff RR, Jordan BH, Babu SS. Development of coatings for ultrasonic additive manufacturing sonotrode using laser direct metal deposition process. Oak Ridge, TN (United States): Oak Ridge National Lab. (ORNL); 2016. Technical Report.
[11] Sridharan N, Cakmak E, Dehoff RR. Microstructure evolution during laser direct energy deposition of a novel Fe-Cr-Ni-WB hardfacing coating. Surf Coat Technol 2019;358:362–70.
[12] Smith RT. Development of a nitrogen-modified stainless-steel hardfacing alloy. The Ohio State University; 2015 [Ph.D. thesis].
[13] Rosakis AJ, Mason JJ, Ravichandran G. The conversion of plastic work to heat around a dynamically propagating crack in metals. J Mech Behav Mater 1993;4:375–86.
[14] Knysh P, Korkolis YP. Determination of the fraction of plastic work converted into heat in metals. Mech Mater 2015;86:71–80.
[15] Gerberich WW, Martens HE, Boundy RA. Tensile properties of five low-alloy and stainless steels under high-heating-rate and constant-temperature conditions. Pasadena, CA (United States): Jet Propulsion Lab. (JPL); 1962. Technical Report.
[16] Sriraman M, Gonser M, Foster D, Fujii HT, Babu S, Bloss M. Thermal transients during processing of 3003 Al-H18 multilayer build by very high-power ultrasonic additive manufacturing. Metall Mater Trans B 2012;43:133–44.
[17] Ward AA, Zhang Y, Cordero ZC. Junction growth in ultrasonic spot welding and ultrasonic additive manufacturing. Acta Mater 2018;158:393–406.
[18] Hehr AJ. Process control and development for ultrasonic additive manufacturing with embedded fibers. The Ohio State University; 2016 [Ph.D. thesis].

[19] Sriraman MR, Gonser M, Fujii HT, Babu SS, Bloss M. Thermal transients during processing of materials by very high power ultrasonic additive manufacturing. J Mater Process Technol 2011;211:1650–7.
[20] Lolla T, Cola G, Narayanan B, Alexandrov B, Babu SS. Development of rapid heating and cooling (flash processing) process to produce advanced high strength steel microstructures. Mater Sci Technol 2011;27:863–75.
[21] SAE-AISI 4130 (SCM430, G41300) Cr-Mo Steel, https://www.makeitfrom.com/material-properties/SAE-AISI-4130-SCM430-G41300-Cr-Mo-Steel, 2020-05-30.
[22] Lee SS, Kim TH, Hu SJ, Cai WW, Abell JA, Li J. Characterization of joint quality in ultrasonic welding of battery tabs. J Manuf Sci Eng 2013;135:021004.
[23] Wu X, Liu T, Cai W. Microstructure, welding mechanism, and failure of Al/Cu ultrasonic welds. J Manuf Processes 2015;20:321–31.